Journal of
Marine Science and Technology

Volume 2 | Issue 1 Article 7

The Use of AC and DC Methods for Corrosion Monitoring of Reinforced Concrete Members in Marine Environment

R. Huang
Department of Harbor and River Engineering

W.D. Yeih
Department of Harbor and River Engineering

J.J. Chang
Department of Harbor and River Engineering

C.C. Yang
Institute of Materials Engineering National Taiwan Ocean University Keelung 20224, Taiwan, Republic of China

Recommended Citation
Huang, R.; Yeih, W.D.; Chang, J.J.; and Yang, C.C. (1994) "The Use of AC and DC Methods for Corrosion Monitoring of Reinforced Concrete Members in Marine Environment," *Journal of Marine Science and Technology*: Vol. 2: Iss. 1, Article 7.
DOI: 10.51400/2709-6998.2488
Available at: https://jmstt.ntou.edu.tw/journal/vol2/iss1/7

Journal of Marine Science and Technology. Vol. 2, No. 1, pp. 53-59 (1994)

THE USE OF AC AND DC METHODS FOR CORROSION MONITORING OF REINFORCED CONCRETE MEMBERS IN MARINE ENVIRONMENT

R. Huang, W.D. Yeih, J.J. Chang

Department of Harbor and River Engineering

C.C. Yang

Institute of Materials Engineering
National Taiwan Ocean University
Keelung 20224, Taiwan, Republic of China

Key words: corrosion, concrete, AC impedance method, DC method, marine envirnoment.

ABSTRACT

Reinforced concrete is the most common engineering material for civil structures. The durability of the concrete structures depends mainly on the corrosion of steel reinforcement. In general, concrete produces an alkaline environment for steel which passivates it, so preventing corrosion. Provided this passivity is maintained, no problem should arise with steel reinforcement. However, in certain environment, chloride ions can locally destroy very protective passive film of reinforcement even though concrete is still alkaline. This paper presents the corrosion results of reinforcing steel in concrete members in marine environment using the AC impedance technique and DC method.

INTRODUCTION

The corrosion of steel reinforcement may result in severe degradation of concrete such as spots, cracks, and spalling. The durability of concrete is mainly dependent on the corrosion behavior of rebars. The electrochemical changes of steel in concrete occur in the presence of oxygen and moisture. The corrosion monitoring techniques of reinforced concrete are becoming increasing important in order to diagnose the corrosion behavior of rebars and to obtain information for corrosion prevention. Many researchers [1- 4] have focused on the application of electrochemical techniques to corrosion measurements. It includes corrosion potential, concrete resistivity measurement, electrical resistance measurement, polarization technique, and impedance measurements. Due to the increasing demand of quantification of corrosion rate, the use of AC impedance measurements has been evaluated recently. Electrochemical impedance measurement has been applied to estimate the corrosion behavior of coated metals over a large frequency for several years [5-8]. However, due to the special electrolytic characteristics of the concrete, there exist many difficulties to be solved for developing accurate monitoring techniques. More experiments need to be set up to clarify the difference between the electrochemical analyses.

The use of fly ash as admixture or partial replacement for portland cement is due to energy conservation and cost effectiveness. Most fly ashes, whether low-calcium or high-calcium, contain 60 to 85 percent glass, 10 to 30 percent crystalline compounds [9]. Its particle sizes vary from 1mm to 100mm in diameter. Fly ash can react with the calcium hydroxide of the portland cement to produce C-S-H gel. Fly ash concrete has been applied to civil structures for many years. Recently, many researchers have paid attention to another pozzolan - silica fume [10-13].

The objective of this paper is to present the influence of various parameters of the concrete mix on the electrochemical properties of the embedded reinforcement using DC and AC techniques.

EXPERIMENTAL PROGRAM

Mix Proportions and Specimen Details

Details of mortar mixes are given in Table 1. Test variables include the water/cement ratio, the percentage of replacement and the type of pozzolans. The control mortar mix C5 was proportioned by weight 1:2.75 with a water/cement ratio of 0.5. Other specimens were mixed with type I portland cement and the water/cementitious material ratios were 0.5, 0.6 and 0.7. Cement replacements by fly ash and silica fume were 7.5, 15 and 30 percent by weight of total cementitious content. Microsilica was used in the form of undensified solids. Six cylindrical mortar specimens of dimension 50 × 100 mm were cast for each mix with the replicate #4 rebar positioned in the center. The average thickness of mortar coverage was 20mm. Cylindrical surface was kept unsealed while top surface was insulated with epoxy-tar paint. The surface of deformed rebars were machined and polished with 400 grit emery paper, washed with acetone prior to casting the specimens. Specimen configuration is presented in Fig. 1.

Materials

Medium carbon steel rebars of 10mm-diameter is used and the chemical composition of steel is given in Table 2. Class F low calcium fly ash was supplied by Taiwan Power Station. The properties of fly ash and silica fume are given in Table 3.

Test Procedure

Cylindrical specimens were immersed in artificial sea water after 28-day moist curing. Artificial sea water was prepared according to the specification of ASTM D1141-75. Corrosion potential and polarization resistance were monitored using a Nichia model G1001 potentiostat as a ramp generator. A typical three-electrode system was applied for electrochemical measurements.

Table 1. Detail of Mixes

Mix No.*	Cement (g)	Sand (g)	Fly Ash (g)	Silica Fume (g)	Water (g) Ratio	Water/ Cementitious
C5	1000	2750	-	-	500	0.5
F5A	700	2750	300	-	500	0.5
F5B	850	2750	150	-	500	0.5
S5B	850	2750	-	150	500	0.5
S5C	925	2750	-	75	500	0.5
C6	1000	2750	-	-	600	0.6
F6A	700	2750	300	-	600	0.6
F6B	850	2750	150	-	600	0.6
S6B	850	2750	-	150	600	0.6
S6C	925	2750	-	75	600	0.6
C7	1000	2750	-	-	700	0.7
F7A	70	2750	300	-	700	0.7
F7B	850	2750	150	-	700	0.7
S7B	850	2750	-	150	700	0.7
S7C	925	2750	-	75	700	0.7

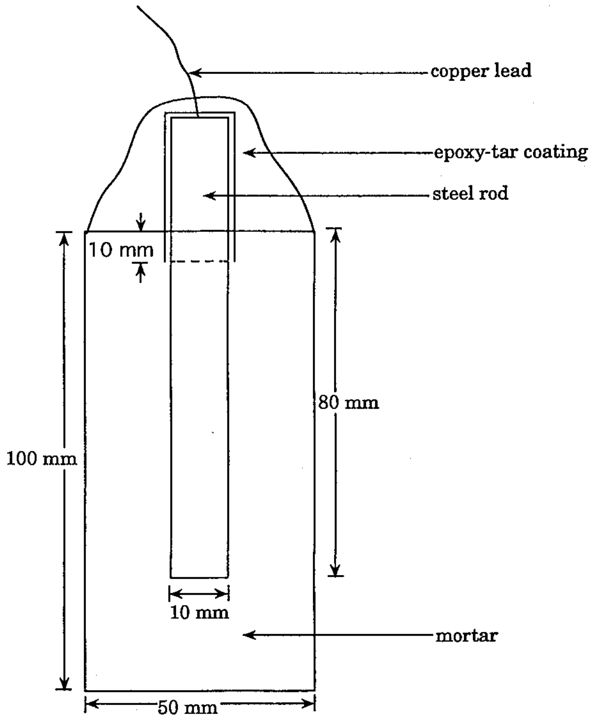

Fig. 1. Configuration of Mortar Specimens.

Table 2. Chemical Composition of Medium Carbon Steel Bar

Element	C	Cu	Si	Mn	P	S
wt %	0.36	0.23	0.20	0.61	0.04	0.025
Element	Ni	Cr	Mo	Sn	Fe	
wt %	0.11	0.12	0.01	0.02	balance	

Table 3. Chemical Composition of Fly Ash and Silica Fume

Chemical Composition	Fly Ash Silica	Fume
SiO_2+Al_2O_3+Fe_2O_3 (%)	86.94	95
SiO_2 (%)	----	94
C (%)	----	1.5
Fe_2O_3 (%)	----	0.4
Al_2O_3 (%)	----	0.6
CaO (%)	0.45	0.3
MgO (%)	0.40	0.8
K_2O (%)	0.27	0.5
Speicfic Weight	2.06	2.09
Water Content (%)	0.53	0.5
Loss of Ignition (%)	7.50	1.5

The electrodes consisted of the steel rebar electrode, a counter electrode and a saturated calomel reference electrode (SCE). Calibration was conducted in accordance with ASTM G5-78 and ASTM G59-78 before testing. A potential sweep from 5 mV cathodic to 5 mV anodic of corrosion potential was performed at a rate of 0.1mV/sec. The potential (V) versus current (i) curves were obtained from output current. The polarization resistances, Rp, were obtained by drawing the slopes on the V-i curves. In addition, the AC impedance measure-ments were also conducted using a Solartron 1286 ap-paratus. A small amplitude perturbation was applied and impedance was scanned. The phase shift ranged from 10^7 Hz to 0.1 Hz. Seven data were recorded at every decade. Open circuit potentials were monitored to determine the DC potentials. The electrochemical measurements of concrete specimens were conducted at 1, 3, 5 and 10 days interval afterwards respectively.

TEST RESULTS AND DISCUSSIONS

Open Circuit Potentials

Effect of Cement Replacement

Corrosion potentials of various mortar specimens in artificial sea water are plotted against immersed time in Figures 2, 3 and 4 for specimens with three different water/cementitious ratios, respectively. Within the range of this study, open circuit potentials of rebars shift to the more positive direction for mixes with a w/c ratios of 0.5 and 0.6. Results for control specimens with a w/c ratio of 0.7 are more negative with longer immersed time witch indicates greater corrosion activity. For mix C7 the open circuit potentials reach the steady states after about 40 day exposure. The OCPs at steady state is about -520mV (SCE). Except C7 and F7C mixes, the OCPs of other specimens in artificial sea water shift to the less active direction. The potentials after 120-day immersion are within the range of -100mV to -300mV(SCE). For mixes with a higher W/C ratio, the cement replacements by fly ash or silica fume has a positive effect on slowing progression toward active potentials. The percentage of cement replacement does not indicate significant effect on open circuit potentials within 120 day exposure. Previous research [14] reported that the probability greater than 90% to have corrosion problem when the measured open circuit potential is less than -350mV ($Cu/CuSO_4$) (-270mV, SCE). Based on this criterion, specimens with a w/c ratio of 0.7 and 30% cement replacement of fly ash commenced to corrode after 100-day immersion. And specimens with a w/c ratio of 0.7 and 7.5% silica fume replacement and 15% fly ash replacement commenced to corrode after 120-day exposure. However, no significant rust was observed on the surface of rebars in the specimens. The corrosion criterion is still not concluded and further study is needed.

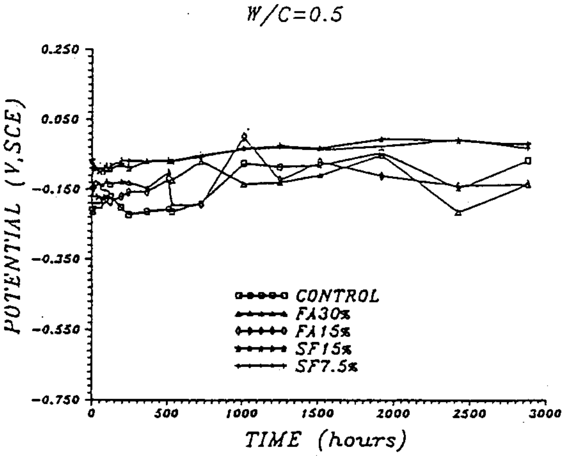

Fig. 2. OCPs vs. Exposure Time Curves for Specimens of w/c=0.5.

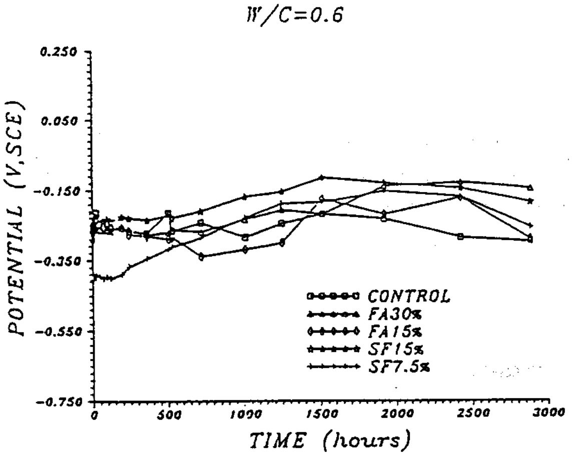

Fig. 3. OCPs vs. Exposure Time Curves for Specimens of w/c=0.6.

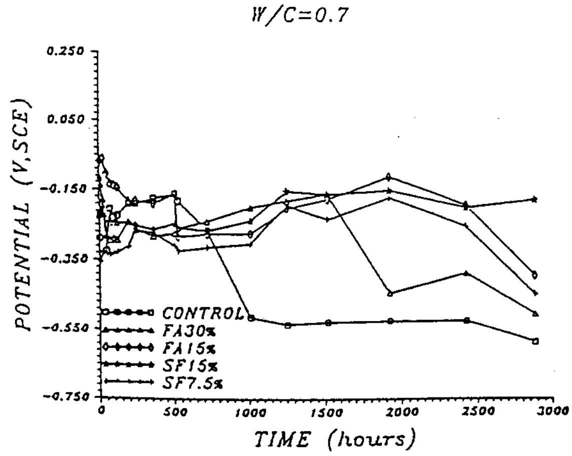

Fig. 4. OCPs vs. Exposure Time Curves for Specimens of w/c=0.7

Effect of Chloride Ions and w/c Ratios

The OCPs vs. exposure time curves of control specimens are plotted in Fig. 5 and 6 for distilled water immersion and artificial sea water immersion, respectively. According to the comparison of two figures, it shows that chloride ions have negative effect on the mixes with high water/cement ratios result in less open circuit potential for specimens immersed in both distilled water and artificial sea water. The same results were also observed in other mixes.

Polarization Resistance (Rp)

DC Polarization Method

The graph of the polarization resistance verse exposure time are plotted and presented in Figures 7 to 9. The Rp of all mixes obtained from ΔE-i curves are within

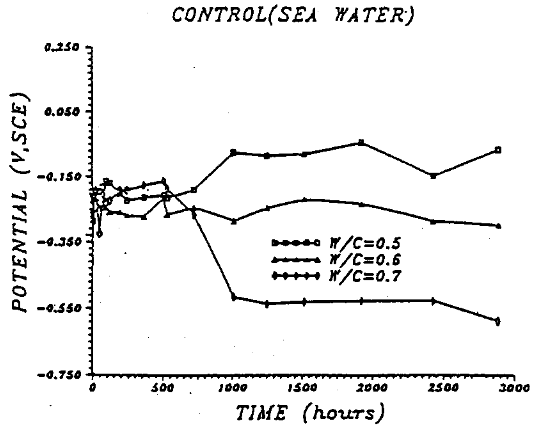

Fig. 5. OCPs vs. Exposure Time Curves for Control Specimens Exposed in Distilled Water.

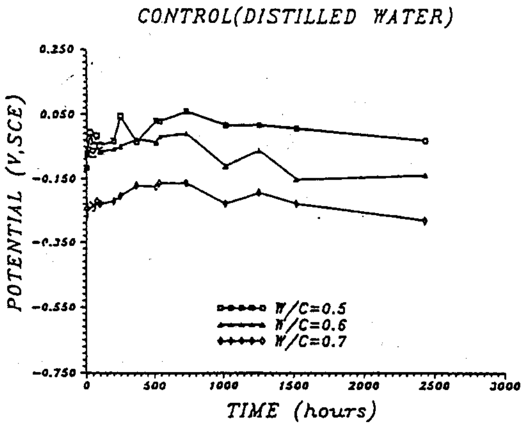

Fig. 6. OCPs vs. Exposure Time Curves for Control Specimens Exposed in Artificial Sea Water.

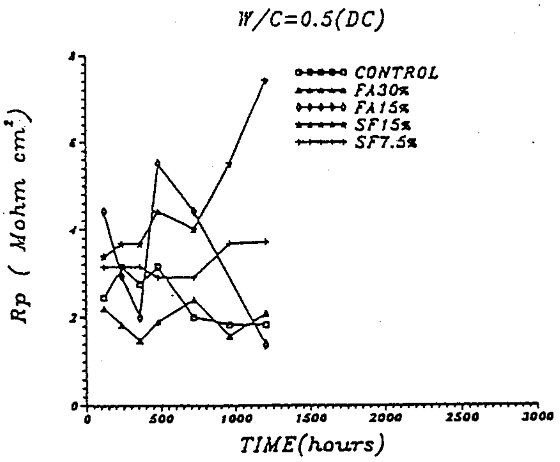

Fig. 7. Polarization Resistance vs. Exposure Time Curves (w/c=0.5).

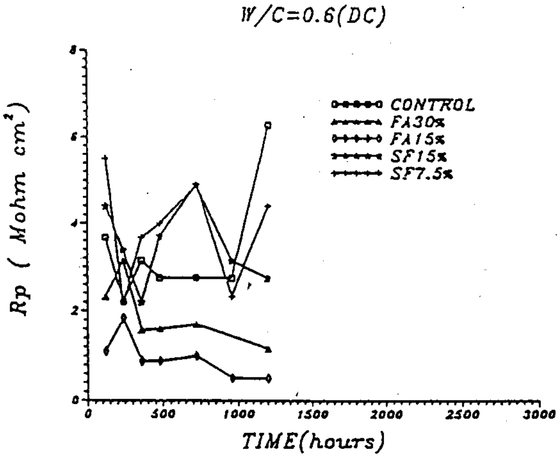

Fig. 8. Polarization Resistance vs. Exposure Time Curves (w/c=0.6).

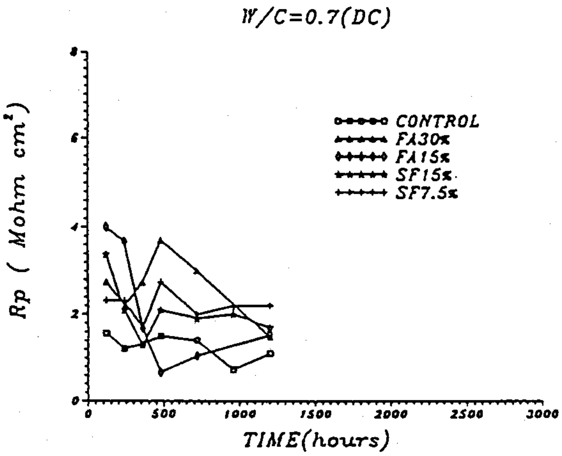

Fig. 9. Polarization Resistance vs. Exposure Time Curves (w/c=0.7).

Table 4. Instantaneous Corrosion Rate of Rebars in Concrete After Immersed in Artificial Sea Water for 1,200 Hours

unit:mpy

W/C=0.5	Control	FA 30%	FA 15%	SF 15%	SF 7.5%
DC Impedance Method	0.0066	0.0057	0.0087	0.0016	0.0032
AC Impedance Method	0.515	0.335	0.320	0.124	0.186
W/C=0.6	Control	FA 30%	FA 15%	SF 15%	SF 7.5%
DC Impedance Method	0.0019	0.0103	0.0240	0.0044	0.0027
AC Impedance Method	0.524	0.412	0.352	0.143	0.263
W/C=0.7	Control	FA 30%	FA 15%	SF 15%	SF 7.5%
DC Impedance Method	0.0110	0.0082	0.0079	0.0071	0.0055
AC Impedance Method	0.455	0.655	0.627	0.165	0.353

the range 1×10^6 ohm•cm^2 to 7×10^6 ohm•cm^2 for all mixes. Because there exists a relationship of inverse proportion between Rp and corrosion current density, it appears that the use of silica fume in mortars has a positive effect on the corrosion resistance the corrosion rates of rebars are tabulated in Table 4. Potential drops due to electrolyte resistance in the mortar mixes were not compensated in the measurement. The corrosion rate may be misled by use of DC technique.

AC Impedance Method

For eliminating the IR drop effect and obtaining more accurate polarization resistance, AC impedance technique was applied in this study. A typical com-plex impedance plot is presented in Figures 10. The polarization resistance obtained from Nyquist plots are given in Figures 11 to 13 for various mixes and w/c ratios. It appears that Rp data obtained from the DC technique are much higher than those obtained from AC impedance plots. This is due to the effect of IR drop. Therefore, the use of DC data may underestimate the corrosion rate of rebar in concrete.

Based on the previous study [12], the corrosion current density can be computed as

$$i_c=\frac{\beta_a\cdot\beta_b}{2.303(\beta_a+\beta_b)}\times\frac{1}{R_P}=B\times\frac{1}{R_P}$$

, where a commonly assumed constant value for B is 0.026. The corrosion rates of rebars ard presented in Table 4.

Comparing the OCP results with Rp data for mix C7, it seems to suggest that the rebar starts to corrode at $i_c=2.16\times10^{-5}$ Amp/cm^2 or a corrosion rate of 9.8 mpy. For other mixes, the same conclusions can be drawn from the results of this study.

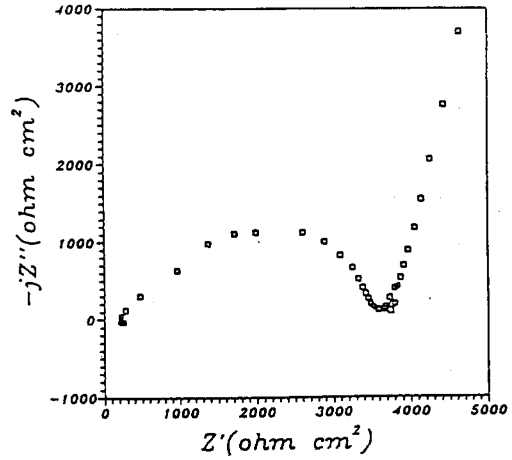

Fig. 10. Typical Complex Impedance Plot.

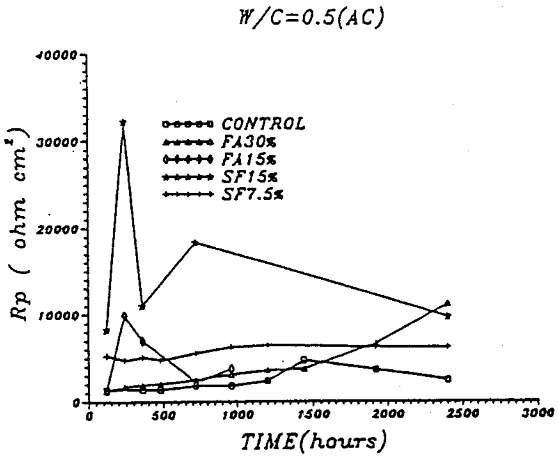

Fig. 11. Polarization Resistance vs. Exposure Time Curves (w/c=0.5).

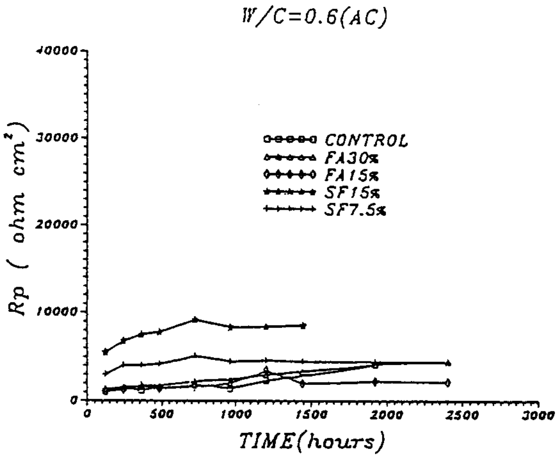

Fig. 12. Polarization Resistance vs. Exposure Time Curves (w/c=0.6).

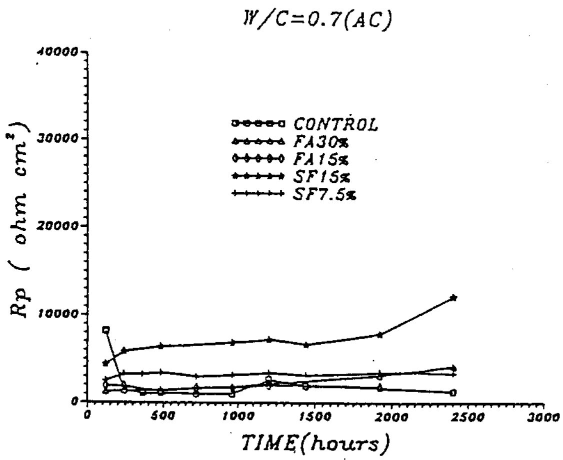

Fig. 13. Polarization Resistance vs. Exposure Time Curves (w/c=0.7).

SUMMARY AND CONCLUSION

1. The potentials of the rebars in concrete decrease as the water/cement ratios increase. And, the use of microsilica as cement replacement material may increase the potential.
2. Chloride environment significantly affects the corrosion resistance of mortars with higher water/cement ratios.
3. The open circuit potentials represent the tendency of oxidation of the composites (concrete and rebar). The decrease of OCPs indicates that the reaction of oxidation accelerates. However, the relationship between the potential and corrosion behavior is not concluded.
4. The use of polarization resistance obtained from DC technique may underestimate the corrosion rate of rebars in concrete. AC impedance data can provide more accurate information about the concrete quality.
5. Replacement of cement by adequate amount of fly ash appears to improve corrosion resistance.
6. Corrosion tendency of rebar in mortar with 7.5% and 15% cement replacement by silica fume are significantly reduced based on OCPs and Rp measurements.

REFERENCES

1. Uhlig, H.H. and Revie, R.W., "Corrosion and Corrosion Control", 3rd edition, Wiley-Interscience, N.Y., 1985.
2. Gabrielli, C., "Identification of Electrochemical Processes by Frequency Response Analysis", Solarton Instrumentation Group, 1980.
3. ASTM C876-87, "Standard Test Method for Half-Cell Potential of Uncoated Reinforcing Steel in Concrete".
4. Hope, B.B., *et al.*, "Corrosion Rates of Steel in Concrete", Cement and Concrete Research, Vol. 16, No. 5, p. 771, 1986.
5. Scantlebury, J.D., Ho, K.N. and Eden, D.A., "Impedance Measurements on Organic Coating on Mild Steel in Sodium Chloride Solutions", ASTM STP 727, ASTM Philadelphia, Pennsylvania, p.187, 1981.
6. Pebere, N., *et al.*, "Evaluation of Corrosion Performance of Coated Steel by the Impedance Technique", Corrosion Science, Vol. 29, No. 9, p. 1073, 1989.
7. Kending, M., Mansfield, F. and Tsai, S., "Determination of the Long Term Corrosion Behavior of Coated Steel with A.C. Impedance Measurements", Corrosion Science, Vol. 23, No. 4, p. 317, 1983.
8. Dra žic, D.M., Miskovic-Stankovic, V.B., "The Determination of the Corrosion Behavior of Polymer-Coated Steel with A.C. Impedance Measurements", Corrosion Science, Vol. 30, No. 6/7, p.575, 1990.
9. Metha, P. K., "Concrete-structure, Properties and Materials", Prentice-Hall, Inc., pp.269-270, 1986.
10. Chatterjii, N., Thaulow, N. and Christensen, P., "Pozzolanic Activity of Byproduct Silisa Fume from Ferrosilicon Production", Cement and Concrete Research, Vol. 12, pp.781-784, 1982.
11. Grufzeck, M.W., Atkinson, S. and Roy, D.M., "Mechanism of Hydration of Condensed Silica Fume in Calcium Hydroxide Solution", ACI, Special Publication, SP-79, Vol. 2, Aug. 1983.
12. Diamond, S., "Effect of Microsilica on Pore Solution Chemistry of Cement Pastes", J. of American Concrete Institute, Vol. 66, No. 5, May 1983.
13. Lessard, S., Aitcin, P.C. and Regourd, M., "Development of a Low Heat of Hydration Blended Cement", ACI, Special Publication, SP-79, Vol. 2, Aug. 1983.
14. "Annual Book of ASTM Standard", secation 4, Construction, Vol.04.02, p.560, 1983.
15. Mangat, P.S. and Molloy, B.T., "Influence of PFA,

Slag and Microsilica on Chloride Induced Corrosion of Reinforcement in Concrete", Cement and Concrete Research, Vol. 21, No. 5, pp. 819-834, 1991.